Journal of Alloys and Compounds 500 (2010) 49–55

Contents lists available at ScienceDirect

Journal of Alloys and Compounds

journal homepage: www.elsevier.com/locate/jallcom

Analysis of thickness dependence on the electrical properties of tin dioxide films in the presence of LPG gas

Sandipan Ray [b,*], P.S. Gupta [a], Gurdeep Singh [b]

[a] Department of Applied Physics, I.S.M.U., Dhanbad, Jharkhand, India
[b] Department of Environmental Science and Engineering, I.S.M.U., Dhanbad, Jharkhand, India

ARTICLE INFO

Article history:
Received 23 January 2010
Received in revised form 6 March 2010
Accepted 8 March 2010
Available online 1 April 2010

Keywords:
Thin films
Sol–gel processes
X-ray diffraction

ABSTRACT

Chloride-based inorganic salt was used to prepare multiple layered tin dioxide thin films by sol–gel method. The deposited films were subjected to SEM, XRD and optical studies. Carrier concentrations of the multiple layered films were studied. A comparative analysis of both undoped and Pd-doped SnO_2 multilayered films has been done in the presence of LPG gas to investigate the possibility of their usage as LPG gas sensors.

1. Introduction

Liquefied petroleum gas (LPG) is the most common cooking fuel in urban areas. It comprises mainly two hydrocarbons – propane (60%) and butane (40%). Accidental fire and bursting of LPG gas cylinders due to leakage are the major risks involved in its usage for cooking purposes. Such accidents generally happen when people are unaware about the gas leakage and unknowingly try to ignite the oven leading to explosion. This calls for the requirement of a room temperature LPG gas detector to avoid the risks involved in its usage and to ensure a safe and healthy environment. ZnO and SnO_2 are the most commonly used metal oxides towards detection of hazardous gases. We have chosen SnO_2 for our field of work.

SnO_2 is an n-type semiconductor material and has a large band-gap of 3.6 eV. It is being widely used as gas sensors for the detection of combustible, toxic and pollutant gases which can harm the environment [1–3]. It can be prepared by several techniques, such as sol–gel method [4–6], chemical vapour deposition, evaporation [7] and sputtering [8,9]. The sol–gel process has recently appeared as a promising technique for preparation of SnO_2 thin films. The benefits of this process are low reaction temperature, uniformity of doping, easy deposition of thin films and low cost. Single or multilayer films prepared by sol–gel method have been studied for various applications by different groups [10]. Amongst them SnO_2 based semiconductors are best tested for the detection of gases [11]. However, a single semiconductor gas sensor is only conditionally suitable for the selective proof of certain gases as it exhibits cross sensitivities to almost all oxidizing and reducing gases. These sensors are also dependent on environmental changes, such as working temperature and humidity.

The present work reports a comparative study of various optical and electrical properties of Pd-doped SnO_2 films for different film thicknesses. These films were further tested for their responses in the presence of LPG gas at room temperature (temperature range between 300 K and 313 K).

2. Experimental details

Reagent grade (Merk) $SnCl_2{\cdot}2H_2O$ was used as precursor material. 8.374 g of $SnCl_2{\cdot}2H_2O$ was dissolved in 100 ml of absolute ethanol. The mixture was refluxed and stirred at 353 K for 3 h and then it was allowed to cool to the room temperature for 1½ h with continuous stirring. A commercial spin coater (Apex SCU 2005) was used for coating the sol on the glass substrates. The speed of the spin coater was fixed at 2100 rpm. Six drops (0.8 ml = 6 drops) of sol were dropped on approximately 1 in. × 1 in. sized clean glass slide. The coated glass slide was air annealed at 673 K for 10 min. The slide was then allowed to cool to the room temperature to produce a transparent SnO_2 film. Using the above procedure multilayered films (with increased film thickness upto twelve-layers) were prepared. Each layer was deposited using the same procedure as before and was annealed with the above mentioned condition. All layers were deposited repeating the same procedure as before and were annealed with the above mentioned condition after every single layer deposition.

These multilayered films were characterized with XRD, optical studies and SEM. Optical studies were done using UV–Vis–NIR Spectroscope and their results were used to calculate the band gap of the films. These undoped films were further characterized for *I*/*V* and hall measurements both in the absence and presence of LPG gas.

To increase the sensitivity, the multilayered films were further doped with palladium. 0.05% solution of palladium chloride was made with ethanol. It was stirred

* Corresponding author. Tel.: +91 9434675174.
E-mail address: write_2_sandipan@yahoo.co.in (S. Ray).

0925-8388/$ – see front matter © 2010 Elsevier B.V. All rights reserved.
doi:10.1016/j.jallcom.2010.03.193

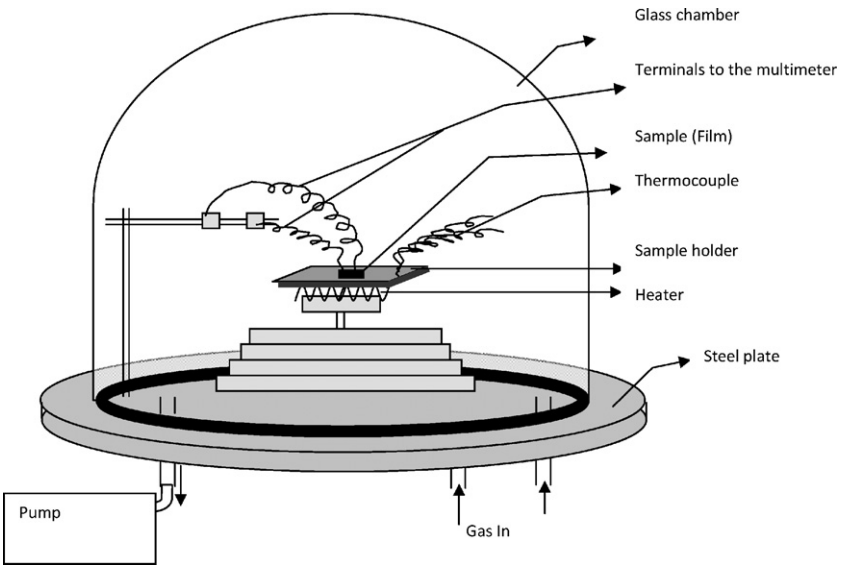

Fig. 1. Schematic diagram of the gas sensing unit used for sensor characteristic measurements.

for 1 h at 323 K and later cooled to the room temperature while stirring. The prepared sol was then spin coated over the same undoped multilayered films to obtain the Pd-doped tin dioxide multilayer samples. The spin coating speed, number of drops applied, the annealing temperature and annealing time are all kept same as those for the undoped samples.

Small pieces of prepared films with dimensions 0.5 cm × 0.5 cm were used for gas sensitivity measurements. It was a two terminal measurement (terminals being fine copper wires of approx 0.05 cm diameter, which were placed 0.3 cm apart on the film surface and fixed with silver paste for better contacts). A digital multimeter (Agilent 34401A) and a constant voltage source (Caddo Programmable DC Power Supply) were used to measure the film's change in the resistance. The measurements were carried out initially in the absence of LPG gas and then in the presence of 1500 ppm of LPG at room temperature for both undoped and Pd-doped SnO_2.

2.1. Experimental setup

The experimental chamber (Fig. 1) used for gas sensitivity analysis of the prepared films consist of a steel base with three port holes at the base for insertion of more than one gas at the same time. Above the steel base there is a raised sample holder made of copper, which is placed over a heating coil used to raise the temperature of the film. The film that is placed above the sample holder is connected by two probes (fine copper wires of 0.05 cm diameter approx.) which are further connected in series with a Programmable DC Power Supply and a Digital Multimeter. The thermocouple (though not used for this experiment as the paper deals with room temperature sensor) as shown in the diagram keeps track of the rise in temperature of the sensing material. The whole system is covered by a glass chamber fitted with rubber tube at its base to ensure zero leakage from the chamber. The chamber is well developed for controlled variations of the inner atmospheric temperature and pressure for controlled gas sensing analysis.

3. Results and discussion

3.1. XRD studies

The X-ray diffraction patterns for the deposited SnO_2 thin films of single layer and multiple layers were obtained and the results of some representative films (three layered, six layered, ten layered and twelve layered depositions) are shown in Fig. 2.

The undoped films upto three layered SnO_2 (Fig. 2a) showed amorphous nature whereas with increase in film layers, crystalline nature sets in. Reflections from the tetragonal crystallographic phase (cassiterite) of SnO_2 became more defined and progressively more intense and sharp for films with more than five layered depositions. The XRD spectra of films (Fig. 2b–d) show reflections from the (1 1 0), (1 0 1), (2 0 0), (2 1 1) and (3 1 0) planes of SnO_2 for 2θ values of 26.8°, 34.05°, 38.12°, 51.9° and 65.51°, respectively. These results comply with the standard SnO_2 XRD pattern of the JCPDS lines [12] as shown in Fig. 3.

Similar XRD pattern, shown in Fig. 2e–h, has been obtained for palladium coatings over SnO_2 thin films. The Pd-doped three layered SnO_2 film showed amorphous nature. For all the other spectra, the addition of palladium peaks and slight reduction in intensity of the SnO_2 peaks are observed. The XRD spectra for Pd-doped SnO_2 show reflections from the (1 1 0) and (2 2 0) planes of palladium corresponding to the 2θ values of 40.65°, and 72.56° respectively. The predominant peaks for eight layered (Fig. 2c and g) and twelve layered (Fig. 2d and h) films can be explained as the cumulative effect of the annealing temperature and time after every single layer deposition. This shows increase in mean grain size and improved crystallinity.

In order to calculate the particle size of the prepared films, Debye–Scherrer formula was employed on the XRD spectra of eight layered and twelve layered doped SnO_2 films and the required formula is given by

$$d = \frac{0.9\ \lambda}{\beta \cos \theta} \quad (1)$$

where λ is the wavelength of the X-ray employed which in this case is 0.15418 nm for Cu-k_α. β is the FWHM (full-width at half maxima) and θ is the Bragg's angle in degrees. The calculated average particle thickness '*d*' for eight layered and twelve layered Pd-doped SnO_2 films is about 31 nm and 28 nm respectively.

3.2. SEM studies

Surface morphologies obtained through Scanning Electron Microscope (SEM) of undoped and Pd-doped SnO_2 films are shown in Fig. 4. Fig. 4a shows comparatively smoother film surface for three layered undoped SnO_2 which is amorphous in nature (also observed earlier from the XRD spectra). For six layered undoped SnO_2 (Fig. 4b), the film surface does not look much different from that of Fig. 4a. However, with further increase in film thickness i.e. for twelve layered SnO_2 (Fig. 4c), we find considerable roughness on the film surface which indicates increase in grain growth. This can be correlated with the predominant XRD peaks as obtained for the twelve layered SnO_2 (Fig. 2e). Comparatively the SEM images for palladium doped films (Fig. 4d–f) show better surface roughness than the undoped SnO_2 films (Fig. 4a–c) respectively, with even better grain growth. However, the SEM images display two major morphologies – one of them (Pd-doped SnO_2 twelve layered film Fig. 4f) shows particles with particle size (∼) 30–40 nm and the

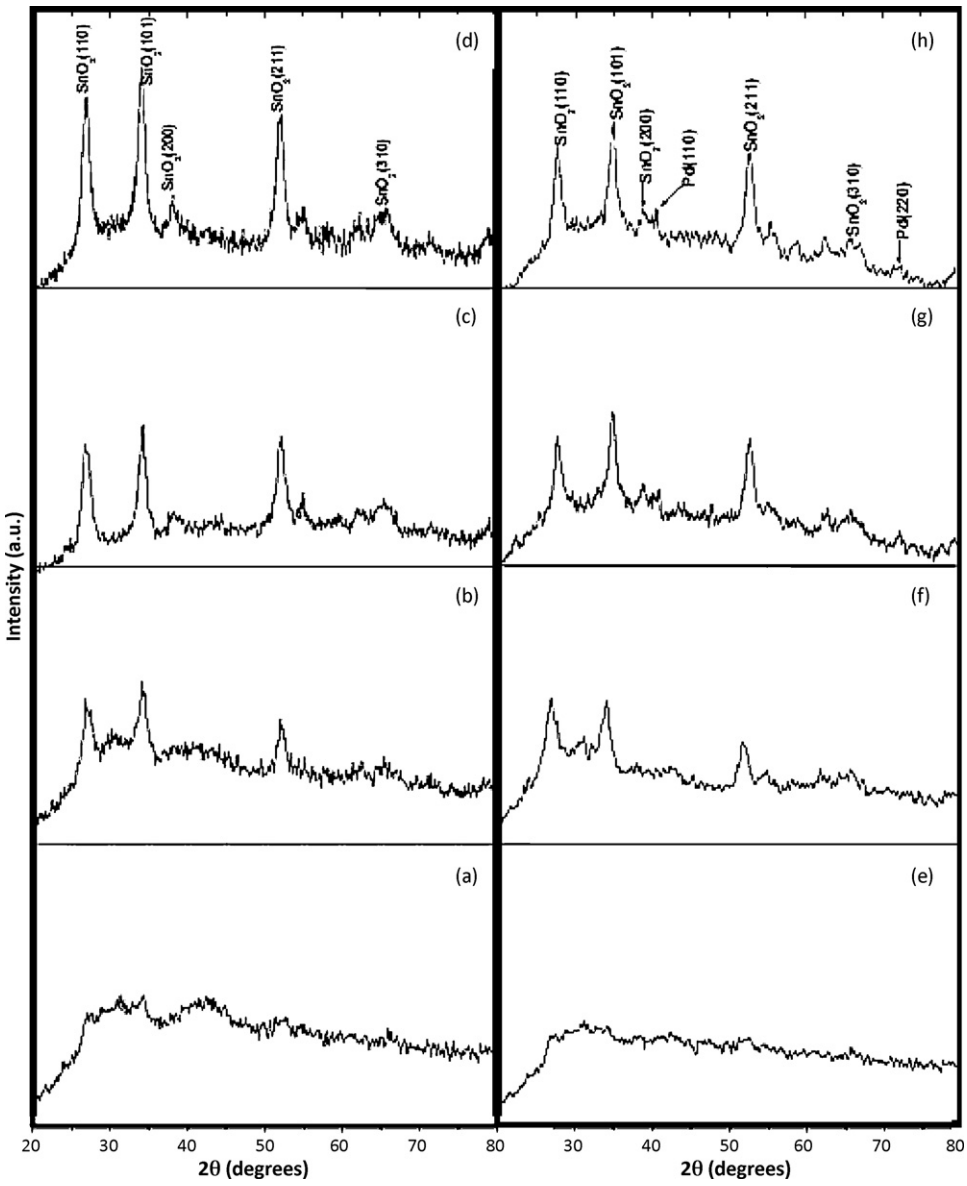

Fig. 2. X-ray diffraction patterns of the SnO_2 thin films with varying deposition layers. For undoped SnO_2 – (a) three layered, (b) six layered, (c) eight layered, and (d) twelve layered and for Pd-doped SnO_2 – (e) three layered, (f) six layered, (g) eight layered, and (h) twelve layered.

other (undoped SnO_2 twelve layered film Fig. 4c) shows slightly bigger clusters consisting of tightly packed small SnO_2 particles with size about 60–80 nm. The nanostructures displayed granules with particle sizes in the range of 30–80 nm and this non-uniform particle size is caused due to the uneven distribution of temperature and mass flow during the synthesis. It is also reflected in the XRD studies (Section 3.1) that the average particle thickness of the prepared eight layered and twelve layered Pd-doped films are about 28 nm and 31 nm respectively. The difference between the values of the particle size obtained by the XRD and SEM are due to the fact that the former is the measure of the diffraction from the crystals, whereas the SEM results correspond to the microscopic view of the deposited sample surface. This prepared SnO_2 particles can easily be termed as 'nano' because the particle size is less than 100 nm.

3.3. Optical studies

The optical studies of the films were carried out using UV–Vis–NIR Spectroscope and the spectral dependence of the transmittance (T) for one layered, three layered, six layered, eight

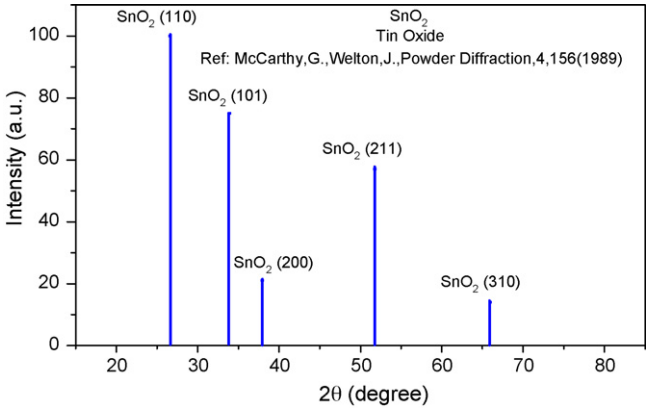

Fig. 3. JCPDS reference lines for SnO_2.

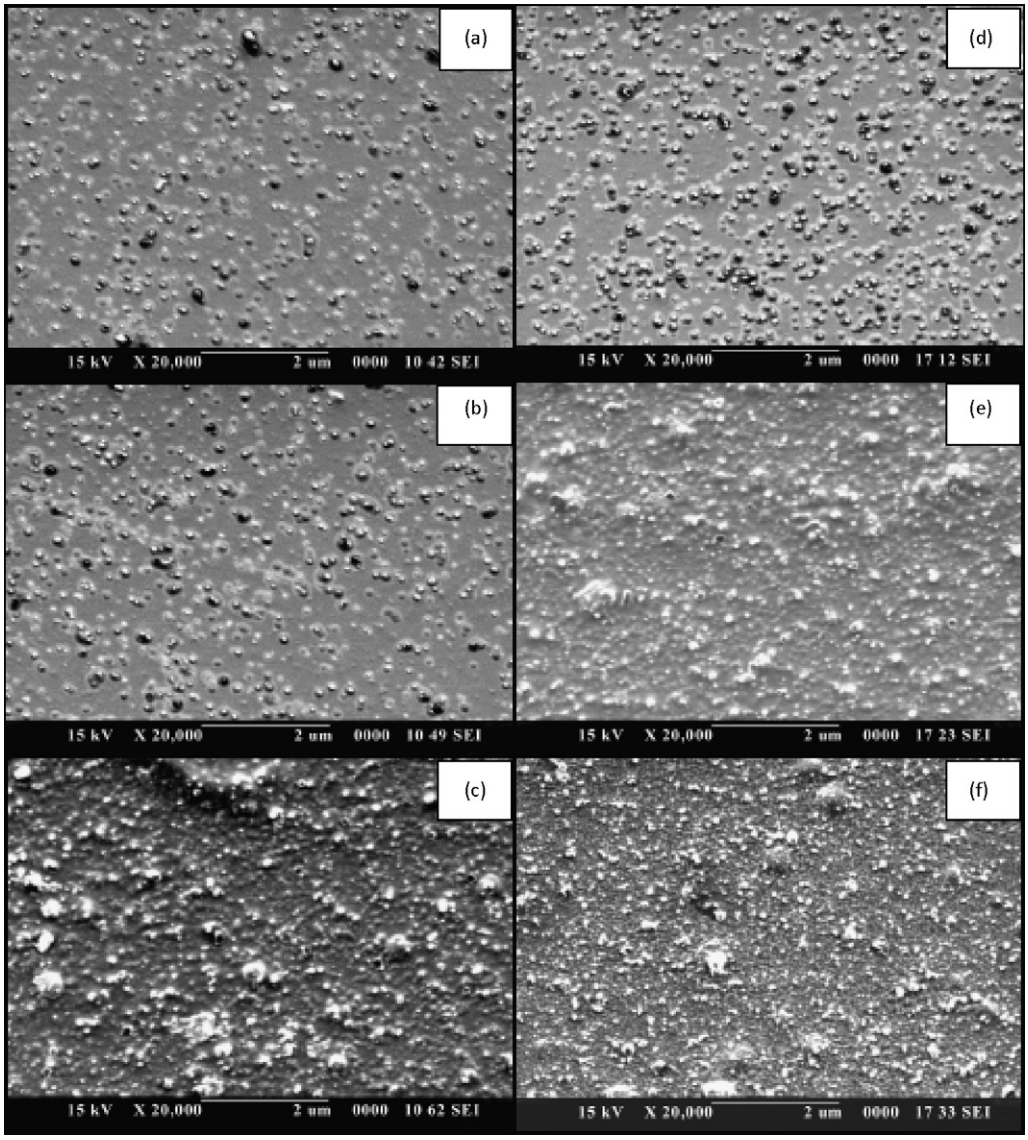

Fig. 4. SEM images of SnO_2 thin films with varying deposition layers. (a) Three layered undoped SnO_2, (b) six layered undoped SnO_2, (c) twelve layered undoped SnO_2, (d) three layered Pd-doped SnO_2, (e) six layered Pd-doped SnO_2, and (f) twelve layered Pd-doped SnO_2.

layered, ten layered and twelve layered films are shown in Fig. 5a and b. The average transmission of the undoped SnO_2 films (Fig. 5a) deposited on glass substrates is more than 80% over the range 450–800 nm. A sharp fall in transmission at about 310 nm is due to the absorption of the glass substrate. The transparency of the films decreases in major portions of the visible range with the addition of layers. This may be due to the built-up thickness which is also clear from the fringes in the transmission spectra. The absorption edge also shifted slightly to higher wavelengths with the increase in film layers. The transmittance falls rapidly in the low wavelength region. With increase in number of layers, the onset of absorption edge becomes less sharp, this may be due to the presence of bigger crystalline sizes and increased scattering due to the surface roughness [11,13].

The optical analysis report for the Pd-doped SnO_2 films is shown in Fig. 5b. With the addition of palladium, the transparency of the films decreased to a great extent as compared to the undoped SnO_2 films. The transmission of the Pd-doped SnO_2 films deposited on glass substrates varied from 5% to 20% over the wavelength range 450–800 nm. It also shows a clear decrease in the average transmittance values with increase in number of film layers along with fall in transmission at about 310 nm due to the absorption of the glass substrate. Fig. 5b shows flat bases on the onset of absorption edges. This may be due to the presence of metallic palladium as well as formation of bigger crystallites and increased scattering due to surface roughness that becomes clear from the SEM images.

The band gaps of these films were calculated from Fig. 5a and b using the formula [14]:

$$\alpha h\upsilon = A(h\upsilon - E_g)^m \quad (2)$$

where α = absorption coefficient; h = Planck's constant; ν = frequency of incident light; E_g = band gap of the material; m = factor governing the direct/indirect, etc. transitions of the electrons from the valence band to the conduction band.

The optical band gaps of the films were obtained by plotting $(\alpha h\nu)^m$ versus $h\nu$ in the high-absorption range followed by extrapolating the linear region of the plots to $(\alpha h\nu)^m = 0$. The linear relations thus obtained for all the samples are most fitted for Eq. (2) with $m = 2$.

The band gap calculated for single layered to twelve layered undoped SnO_2 films varied from 3.76 eV to 3.61 eV and that for Pd-doped SnO_2 it varied from 3.70 eV to 3.43 eV, respectively, which are comparable to that of bulk SnO_2 (band gap = 3.6 eV). The band

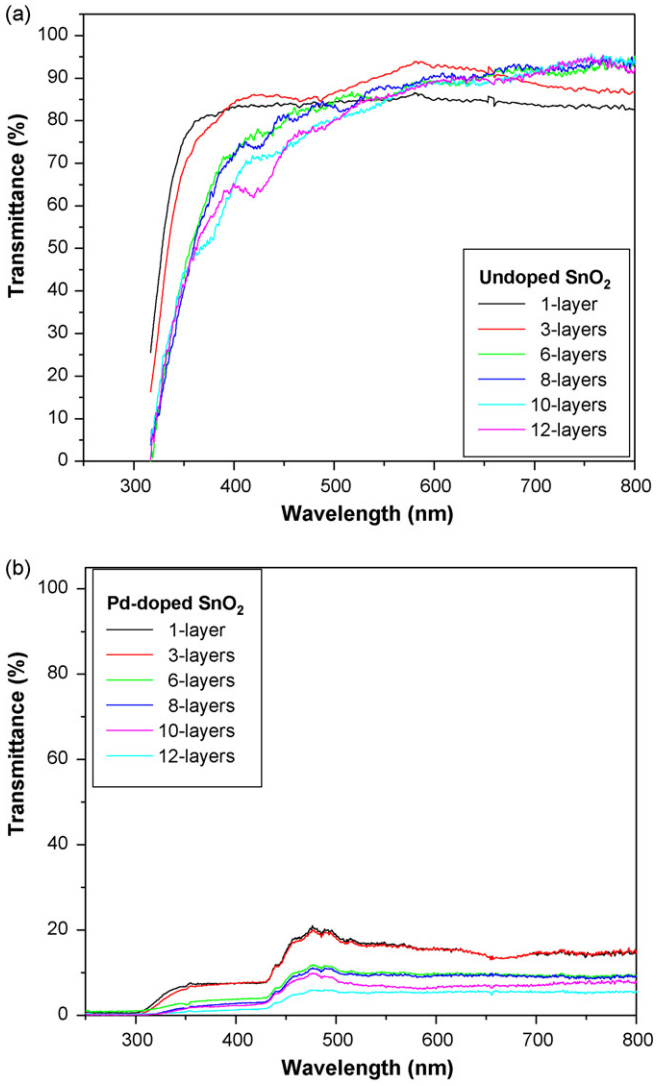

Fig. 5. Optical transmission spectra of multilayered (a) undoped and (b) Pd-doped SnO_2 films annealed at 673 K.

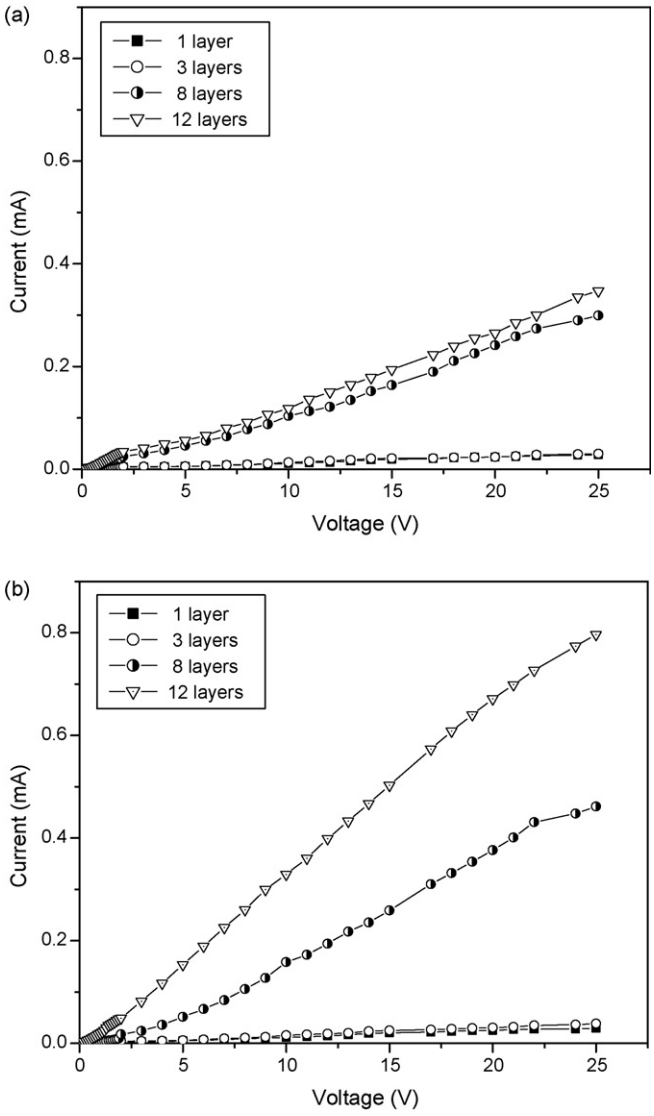

Fig. 6. *I/V* curve for undoped SnO_2 (a) without gas exposure and (b) with LPG gas exposure.

gap was found to decrease considerably for films with increased film thicknesses.

The deposited SnO_2 films' thicknesses were calculated from their optical data using the equation [15]:

$$t = \frac{N_o \lambda_1 \lambda_2}{2(n_1\lambda_2 - n_2\lambda_1)} \quad (3)$$

where N_o = number of oscillations between two extrema and n_1 and n_2 represent the refractive indices of the film at wavelengths λ_1 and λ_2 respectively. The refractive index was obtained from the relation

$$n^2 = \left[\frac{n_a^2 + n_g^2}{2 + 2n_a n_g T_o}\right] + \left[\left\{\frac{n_a^2 + n_g^2}{2 + 2n_a n_g T_o}\right\}^2 - n_a^2 n_g^2\right]^{1/2} \quad (4)$$

where

$$T_o = \frac{T_{max} - T_{min}}{T_{max}.T_{min}}$$

The films' thicknesses were calculated from the above expressions and were found to vary from 0.18 μm to 1.75 μm for single layered and twelve layered undoped SnO_2 films, respectively. After palladium doping, the calculated films' thicknesses ranged between 0.24 μm and 1.80 μm for single layered and twelve layered films, respectively. Film thickness depends upon the preparation techniques (i.e. numbers of drops, drop size, rotation speed of the spin coater, etc.) and hence the thicknesses of the films are not exactly proportional to the number of layers. It has been found to have an error of approximately ±2% after three or four layers of depositions.

3.4. *I/V characteristics*

Figs. 6a and b and 7a and b represent the *I–V* characteristics of undoped and doped SnO_2 films, respectively, in the presence and absence of LPG gas. These characteristic graphs show rise in slopes when the subjected films are exposed to LPG gas. Interestingly, the films show a better sensing pattern with increase in the number of film layers. This can be attributed to the decrease in grain boundary and the increase in grain growth, against the stacking of film layers along with the cumulative effect of the annealing temperature. It provides a larger surface area to interact with the exposed gas. Moreover, the addition of palladium on top of SnO_2 films increases its surface conductivity. The increase in slope in the presence of gas is an indication of the film's ability to sense LPG gas. For representative films of eight and twelve layers, it is observed from the slope differences that the response of their doped films is

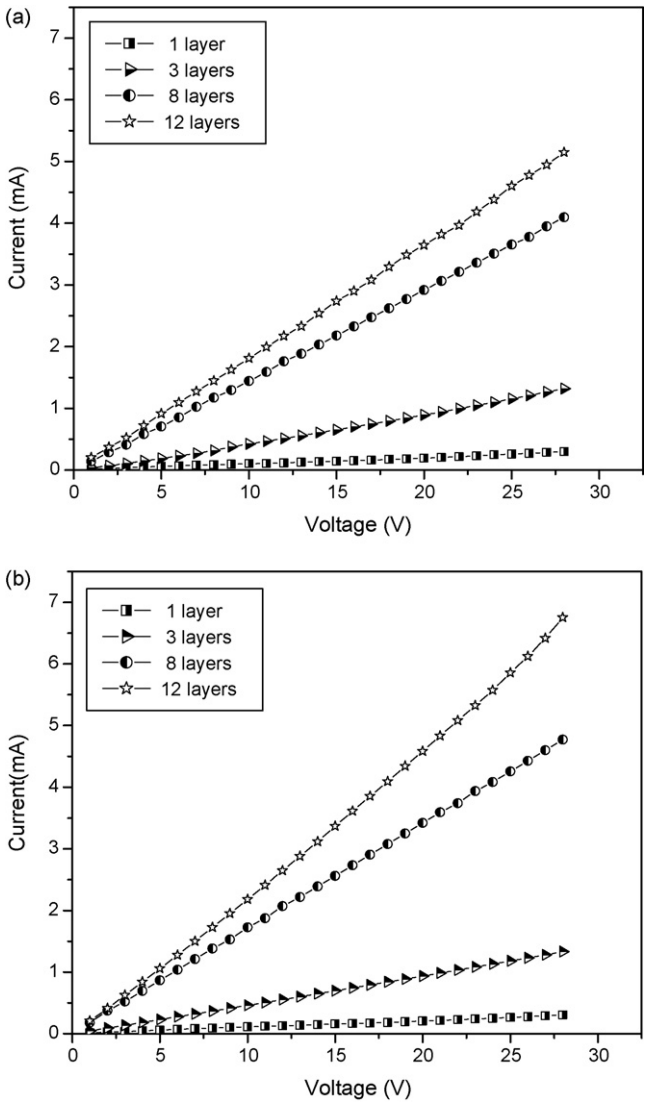

Fig. 7. *I*/*V* curve for Pd-doped SnO_2 (a) without gas exposure and (b) with LPG gas exposure.

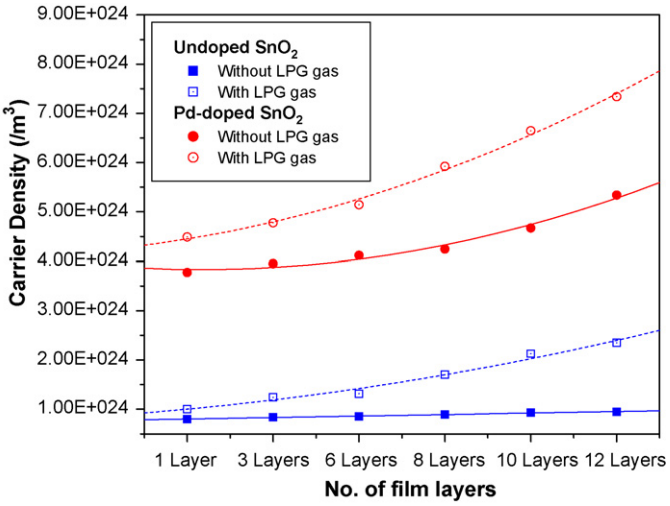

Fig. 8. Variation of carrier densities with increased number of film layers for undoped and Pd-doped SnO_2 films.

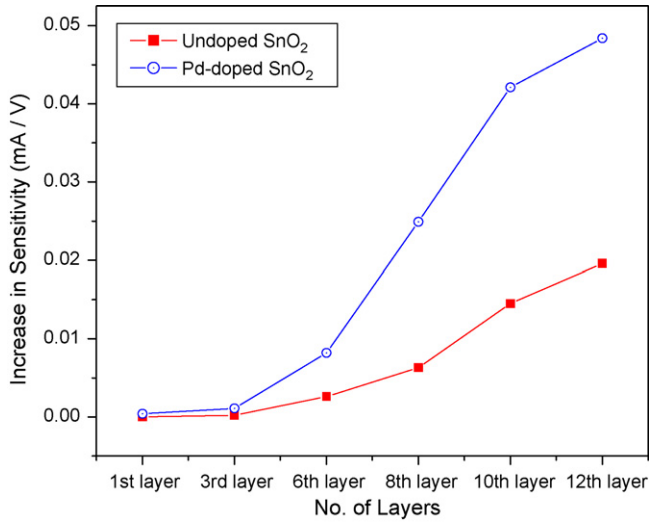

Fig. 9. Sensitivity of SnO_2 to LPG gas with increasing number of film layers.

around three times more than that of their undoped films. Hence, multilayer doped SnO_2 films can be used as an efficient LPG gas sensor.

Hall measurements (at 2000 G magnetic field) have also been carried out for these films which supports the rising trend in the sensing behaviour of these Pd-doped multilayered SnO_2 thin films as observed in the *I*/*V* characteristics. Fig. 8 shows an increase in carrier concentrations with increase in film layers for both undoped and Pd-doped SnO_2 films when exposed to LPG gas. Thus, it shows increase in conductivity, as supported by the increased *I*/*V* characteristic slopes and also by the optical data showing gradual decrease in band gap with increased film thicknesses.

3.5. Gas response

The gas response of SnO_2 films are calculated from their respective *I*/*V* slopes (Figs. 6 and 7). Generally, gas sensitivity (*S*) calculation is done from the formula $S(\%) = \{(R_{air} - R_{gas})/R_{air}\} \times 100$, R_{air} and R_{gas} being the sensor resistance in air and gas at the same temperature [13]. Here we have represented the observed gas response as change in slope ($Slope_{gas} - Slope_{air}$); $Slope_{air}$ being the slope of the *I*/*V* curve in the absence of LPG and $Slope_{gas}$ being the slope of the *I*/*V* curve in the presence of LPG gas. The difference in the slopes is plotted graphically in Fig. 9 to show the response of the prepared films in the presence of 1500 ppm LPG gas.

Due to n-type behavior of SnO_2, the electrical conductivity increased with a reducing gas like LPG. Experimental results show that tin dioxide has a good response to LPG gas. The resistances of SnO_2 films depend on the various oxygen deficient sites present on the film surfaces as well as on the doping level. With little incorporation of palladium onto SnO_2, it resides on the grain boundaries of the films. Palladium doped over the SnO_2 films generate surface states and provides excess electrons to them. The gas response is further enhanced by the buildup of film layers and is evident from the SEM images which show increased surface area for better gas adsorption. It is also evident from the optical data which shows decrease in the calculated band gaps showing better conductivity. However, the gas response tends to saturate with further depositions as observed for twelve layer films, shown in Fig. 9.

4. LPG detection mechanism

The main constituents of LPG are propane, butane and propene. Propene is an unsymmetrical alkene with a double bond. It being

more unstable than propane and butane is better prone to hydrogenation especially in the presence of catalyst like Pd. The *p* electrons as present in propene are weak bonds which are easily broken.

The possible reaction at the SnO_2 active surface, exposed to a reducing gas like LPG may be described as follows:

$$2e^- + 2O = 2O^-;$$

where e^- represents a conduction band electron. Resistance of tin oxide films depends mainly on various oxygen-deficient sites present after deposition as well as on the doping level. The palladium incorporated was found to reside on the grains and at the grain boundaries of SnO_2 films. Presence of Pd in the film generates surface states and provides excess electrons to them. However, in the absence of reducing gas, electrons are removed from the conduction band via reduction of adsorbed molecular oxygen and formation of O^- species. These O^- species on the SnO_2 film surface consequently makes it highly resistive. When LPG is introduced, it reacts with surface oxygen anion (O^-) and electrons are reintroduced into the conduction band. Thus, an increase in the film conductivity is observed. Desorption of these oxygen species at the surface may be due to the possible hydrogenation of propene in the presence of Pd. This transport of electrons due to the breaking of p bonds of propane would culminate in an increase in conductance of the SnO_2 layer significantly in the presence of the LPG gas. This is also reflected in significant increase in carrier concentration upon exposure to LPG. It showed reduction in hall mobility due to the trapping of electrons at the grain boundaries.

5. Conclusion

The present work reports the depositional technique and characterization of multilayered undoped and Pd-doped SnO_2 thin films. Electrical measurements were carried out and it has been found that SnO_2 is a moderate LPG gas sensor at room temperature. Its gas response can be increased with the addition of a catalyzing agent like palladium and can further be improved by the build up of multiple layers.

References

[1] K. Anothainart, M. Burgmair, A. Karthigeyan, M. Zimmer, I. Eisele, Sens. Actuators B: Chem. 93 (2003) 580–584.
[2] G.G. Mandayo, E. Castano, F.J. Gracia, A. Cirera, A. Cornet, J.R. Morante, Sens. Actuators B: Chem. 95 (2003) 90–96.
[3] R.S. Niranjan, K.R. Patil, S.R. Sainkar, I.S. Mulla, Mater. Chem. Phys. 80 (2003) 250–256.
[4] Z.A. Ansari, S.G. Ansari, T. Ko, J.-H. Oh, Sens. Actuators B: Chem. 87 (2002) 105–114.
[5] A. Cabot, J. Arbiol, J.R. Morante, U. Weimar, N. Barsan, W. Gopel, Sens. Actuators B: Chem. 70 (2000) 87–100.
[6] A. Chiorino, G. Ghiotti, F. Prinetto, M.C. Carotta, D. Gnani, G. Martinelli, Sens. Actuators B: Chem. 58 (1999) 338–349.
[7] Y.-S. Lee, O.-S. Kwon, S.-M. Lee, K.-D. Song, C.-H. Shim, G.-H. Rue, D.-D. Lee, Sens. Actuators B: Chem. 93 (2003) 556–561.
[8] L. Jianping, W. Yue, G. Xiaoguang, M. Qing, W. Li, H. Jinghong, Sens. Actuators B: Chem. 65 (2000) 111–113.
[9] P. Santos, A. de Agapito, Thin Solid Films 338 (1999) 276–280.
[10] M. Sharma, R.M. Mehra, Appl. Surf. Sci. 255 (2008) 2527–2532.
[11] S.A. Mahmoud, A.A. Akl, H. Kamal, K. Abdel-Hady, Physica B 311 (2002) 366.
[12] G. Mc Carthy, J. Welton, Powder Diffr. 4 (1989) 156.
[13] A.E. Jiménez-González, J.G. Cambray, Surf. Eng. 16 (2000) 73.
[14] S. Majumder, S. hussain, R. Bhar, A.K. Pal, Vacuum 81 (2007) 985–996.
[15] A. Sarkar, S. Ghosh, S. Chaudhuri, A.K. Pal, Thin Solid Films 204 (1991) 255–264.